Reentrant layering in rare gas adsorption: preroughening or premelting?

Franck Celestini[1], Daniele Passerone[2,3], Furio Ercolessi[2,3], and Erio Tosatti[2,3,4]

[1] *Laboratoire MATOP associé au CNRS, Université d'Aix-Marseille III, Marseille, France*
[2] *International School for Advanced Studies (SISSA-ISAS), I-34014 Trieste, Italy*
[3] *Istituto Nazionale di Fisica della Materia (INFM), Italy*
[4] *International Centre for Theoretical Physics (ICTP), I-34014 Trieste, Italy*

The reentrant layering transitions found in rare gas adsorption on solid substrates have conflictually been explained either in terms of preroughening (PR), or of top layer melting-solidification phenomena. We obtain adsorption isotherms of Lennard-Jones particles on an attractive substrate by off lattice Grand Canonical Monte Carlo (GCMC) simulation, and reproduce reentrant layering. Microscopic analysis, including layer-by-layer occupancies, surface diffusion and pair correlations, confirms the switch of the top surface layer from solid to quasi-liquid across the transition temperature. At the same time, layer occupancy is found at each jump to switch from close to full to close to half, indicating a disordered flat (DOF) surface and establishing preroughening as the underlying mechanism. Our results suggest that top layer melting is essential in triggering preroughening, which thus represents the threshold transition to surface melting in rare gas solids.

Rare gas solid surfaces and films provide an important testing ground for a variety of surface phase transitions. Surface melting [1], roughening [2], and more recently preroughening (PR) [3] have been identified or at least claimed at the free rare gas solid-vapor interface. Layering transitions of thin rare gas films on smooth substrates have given rise to a wide literature [4]. The discovery of reentrant layering (RL) – the unexpected disappearance and subsequent reappearance (well below the roughening temperature) of layering steps in adsorption isotherms on smooth substrates [5,6] – has led to a debate [7]. One possible explanation is PR, a phase transition which takes a surface from a low-temperature "ordered flat" state, with essentially full surface coverage ($T < T_{PR}$), to a high temperature "disordered flat" (DOF) state, with half coverage, and a network of meandering steps ($T > T_{PR}$). Layering would disappear at PR, but re-enter in the DOF state [3,8]. The competing explanation is based on the possibility of a melting-solidification-melting sequence in the top surface layer, similar to that seen for increasing temperature in canonical molecular dynamics simulations [9]. In this picture, RL would result directly from a layer-promotion-driven melting of the top surface layer, and the subsequent advance of a solid-liquid interface [7]. Both approaches appear to capture some important physics, but both also have problems. The non-atomistic statistical mechanics lattice models provide, in presence of an attractive substrate potential, an overall adsorption phase diagram with zig-zag lines of heat capacity peaks (whose behavior has been called "zippering" [10]) which are centered at T_{PR} and strikingly resemble experimental observations [6]. Because they contain PR, the models can naturally explain why the coverage jump across RL should be about half a monolayer, as seen in ellipsometry [5] and in X-ray measurements [11]. However, they fail to account for continuous atom dynamics, in particular melting, and it remains unclear how bad the total

neglect of these aspect might be at these relatively high temperatures. In Ar (111), RL takes place near $69K$, not too far from melting at $T_m = 84K$. By contrast, the atomistic canonical simulation approach does not suffer from that problem, and can describe quite well all the surface degrees of freedom, including thermal evolution of each surface layer from solid to liquid. It finds, realistically, that top-layer surface melting seems to be setting on precisely near the RL temperature. However, it does not explain the half layer coverage jump across RL. A crucial underlying difficulty of this approach lies in the fixed particle number – a difficulty which the lattice models, being naturally grand canonical, do not encounter. In this situation Grand Canonical Monte Carlo (GCMC) atomistic simulation should be the method of choice, applied since long ago [12] to describe adsorption, albeit of a single monolayer. Recently, we demonstrated how a free rare gas (111) surface can be realistically simulated by GCMC with a Lennard-Jones potential, and found indications that PR is indeed incipient at $0.8\,T_m$ [13]. That work however remained incomplete, because a full equilibrium stabilization of the grand canonical surface proved to be increasingly hard with increasing temperature, and failed above $0.8T_m$, where a value of μ that would cause neither decrease nor increase of the total particle number could no longer be found.

In this Letter we present results of a fully equilibrated realistic GCMC simulation of multilayer rare gas adsorption on a flat attractive substrate. In this case, the substrate potential naturally provides the necessary stabilization for the system. We obtain realistic adsorption isotherms, whose main features compare directly with experiment. Reentrant layering is recovered, and layer occupancies confirm its association with a DOF surface and thus with PR. At the same time however, surface diffusion and pair correlations show that while the virtually full monolayer below T_{PR} is solid, with only a gas

of adatoms and vacancies, the half-full monolayer found above $T_{\rm PR}$ is made of a 2D liquid islands (even if in a strong periodic potential). A new picture emerges, where the fractional monolayer melting, besides opening the way to surface melting, is also a key element favoring the preroughening of these surfaces.
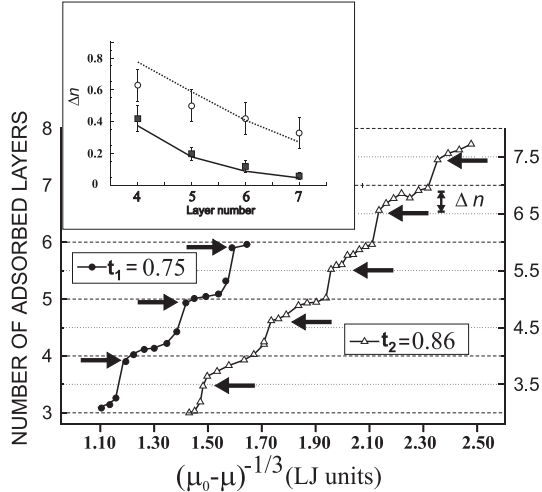

FIG. 1. Calculated adsorption isotherms for $t_1 = 0.75$ (0.53ϵ) and $t_2 = 0.86$ (0.61ϵ), respectively below and above reentrant layering ($t = 0.83$). Arrows indicate that at t_1 the layering steps lead to roughly integer coverage, while at t_2 they lead to roughly half-integer coverage. The abscissa for isotherm t_2 is shifted by 0.4. Inset: amplitude of the plateau breadths between two jumps in the t_2 isotherm. Circles: this simulation. Squares: extracted from Ar/graphite data [5]. Full line: model fit to experimental breadths, as described in the text, with $c/k = 1200$. Dashed line: prediction of the same model, for a 10-fold enhanced substrate attraction γ.

We simulate adsorption by classical GCMC, implementing small displacement moves (m), creations (c), and destructions (d) with relative probabilities $\alpha^{(m)} = 1 - 2\alpha$ and $\alpha^{(c)} = \alpha^{(d)} = \alpha$. Small moves apply to all particles, whereas creation/destruction is restricted to a fixed surface region, about four layers wide, since their acceptance in the fourth layer of this region is already negligible on the entire MC run. In standard bulk GCMC the fastest convergence to the Markov chain is for $\alpha = 1/3$ [14]. For our surface geometry and our potential, the optimal value of α is found to be small, of order 10^{-3} (the precise value depending on the outer layer population relative to the total), as needed to allow for a more effective equilibration after each creation/destruction move. Creation and destruction acceptance probabilities were checked explicitly to satisfy the detailed balance. We simulated adsorption of atoms interacting via the (12,6) Lennard-Jones potential truncated at 2.5σ. The bulk fcc triple point temperature T_m of this model is $\sim 0.7\epsilon$ [15] (note that pressure dependence is negligible, i.e. $P_m/T_m(dT_m/dP) \simeq 2 \times 10^{-4}$ for Ar), and we will from now on switch notation to a re-

duced temperature $t = T/T_m$. The substrate was taken to be flat and unstructured. Periodic boundary conditions were assumed along the x and y directions, with a reflecting wall along z, placed way above the surface. Interactions between atoms and substrate were also of the Lennard-Jones form, giving rise to a laterally invariant (3,9) potential $V(z) = A(B/z^9 - C/z^3)$, with $A = 40\pi/3$, $B = 1/15$ and $C = 1/2$, the latter $\simeq 10$ times larger than the true Ar/graphite value, so as to avoid the stabilization problems encountered previously with the free solid-vapor interface [13]. The (xy) simulation box size was of 22×23 σ units and a full fcc layer contained $N_l = 480$ atoms. We focused on two temperatures, $t_1 = 0.75$ and $t_2 = 0.86$, (respectively below and above the RL temperature $t \simeq 0.83$), where we obtained full and converged adsorption isotherms. For each temperature we increased the chemical potential μ (i.e., increased the pressure of the fictitious perfect gas in contact with the system) by intervals of $\simeq 0.02\epsilon$ and waited for stabilization of both total energy and particle number. Generally half a million Monte-Carlo (MC) moves/particle were sufficient to reach equilibrium. Then 30 to 50 uncorrelated configurations were generated from a subsequent half million MC moves and analyzed.

Fig. 1 shows the calculated adsorption isotherms – the number of adsorbed layers versus $(\mu_0 - \mu)^{-1/3}$ – μ_0 being the saturation chemical potential (where a bulk quantity of matter would condense). At the lower temperature t_1 we find clear layering steps between consecutive integer layers numbers. Analysis of layer occupancies shows that after each coverage jump the first layer is nearly full, with $\simeq 15 - 20\%$ of vacancies, and only few adatoms. In the subsequent plateau the adatom population gradually increases to $\simeq 15 - 20\%$ and vacancies in the first layer are filled, until the next jump suddenly occurs, and so on. Between t_1 and t_2 we generally observed that, as in experiments, the layering steps tended to disappear; however here it became very difficult to obtain a stable surface and thus well defined adsorption isotherms. At the higher temperature t_2 we did recover stability, and we found that layering was again present, but with two important qualitative differences with the low temperature isotherm: coverage was shifted by half a monolayer, and plateaus were broader. Adsorption began at a half-full layer here, and it progressed continuously, leading to a broader plateau, until the next jump to another half integer coverage. We plot in Fig. 1 the t_2 isotherm up to eight adsorbed layers, the maximum thickness before encountering again stabilization problems. The large plateau breadths are clearly due to our strong substrate potential. The film grand potential can be crudely modeled as a periodic part, say $k\cos(2\pi n)$, plus an effective interface repulsion, $c/(2(n - n_0)^2)$ [16], plus a growth term μn (n is the total number of layers). The plateau breadth is thus predicted to decrease asymptotically in the form $\Delta n \simeq 1/(1 + \gamma^{-1}(n - n_0)^4)$, where $\gamma = 3c/(4\pi^2 k)$

measures the strength of the substrate. As Fig. 1 (inset) shows, this law fits well the experimental data, with $c/k = 1200$. It also agrees fairly well with our actual GCMC plateau widths, once γ is increased by the correct factor 10. We also note from Fig. 1 the relatively large compressibility k^{-1} of the half-coverage state with respect to the low-temperature state.
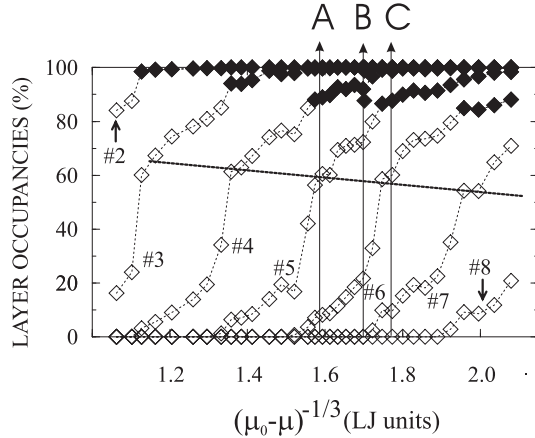

FIG. 2. Occupancies of the different layers versus the chemical potential calculated at $t_2 = 0.86$ (0.61ϵ). White diamonds indicate a liquid-like layer; black diamonds a solid-like layer.

We conclude that our simulation reproduces the basic RL phenomenon, making it possible to probe deeply into its nature. For a better understanding of the layering reentrance, we plot in Fig. 2 the occupancies, at $t_2 = 0.86$, of the different layers for increasing chemical potential. The jumps leading to fractional coverage states are clearly observable. Following each jump (A, layer #5), the coverage increases continuously by a fraction of monolayer, enriching the adatom population, as well as first and second layers, until at (B) the surface (layer #6) is ready for the next jump, leading to (C) where, following the jump, former adatoms (layer #6) increase in density to form a new half layer, and a new adatom layer (#7) is started. We found no trace of the non-monotonic occupancies reported in earlier canonical studies [9]. The top layer occupancy extrapolates to about 50 % for large adsorbate thickness, strongly supporting the identification with a DOF state: an ordinary 2D liquid should display a much higher average lateral density. The occupancies of the three outermost layers (0.1, 0.5, 0.8) for what we thus suppose to describe a realistic DOF state differ somewhat from the simplistic ones expected from lattice models, namely (0.0, 0.5, 1.0). The finding of a DOF surface at t_2, against an ordinary flat surface [occupancies (0.15, 0.85, 1.0)] at t_1 indicates that PR of the free rare gas solid surface must take place in between. This conclusion is also supported by the evidence of DOF phase separation taking place at $t \simeq 0.83$ independently obtained by canonical simulations of the free Lennard-Jones surface [17].
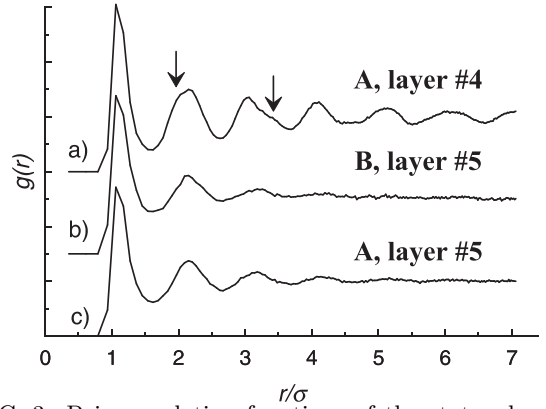

FIG. 3. Pair correlation functions of the states described in the text. a) Arrows indicate shell features of a solid layer; b),c). Absence of shell features indicates liquid layers.

One might thus be led to think that apart from details, the physics is just that dictated by simple SOS models [8]. However, a closer look at our MC configurations reveals that the situation is different, and richer. Following [9] we studied the lateral positional ordering and diffusion coefficients of different layers at the two temperatures by examining pair correlation functions, in particular at $t_2 = 0.86$. For this purpose we carried out two separate canonical molecular dynamics simulations (the diffusion coefficient is ill-defined in a grand canonical simulation), one with an integer layer number, and another with half-integer (no substrate). They were meant to approximate free stable grand canonical surfaces below and above $t_{RL} = 0.83$, and thus chosen with the same coverages ~ 0.5 and ~ 1 of the grand canonical states A and B described earlier. Fig. 3 shows a selection of lateral pair correlation functions $g(r)$ calculated at t_2. Presence of shell-related peaks/shoulders indicates a solid layer, their absence a liquid layer [9]. We see that the top layer is always liquid, but that it solidifies right after being covered by the next half layer. Consider for instance state A in Fig. 2. The upper layer (#6) has 10% of adatoms (a 2D gas), the lower layer (#4) has 20% of vacancies and is solid, but the the middle half filled layer (#5) is liquid. As coverage increases, layer #5 gets denser, but remains liquid until jump B (see Fig. 3). After that, at C, the former adatoms condense into another fluid half layer #6, while at the same time layer #5 solidifies, leading to a surface identical to the starting one except for one extra layer. This picture is close to that suggested by heat capacity studies [6]. It is also similar to that described by canonical simulations [9], differing however in two crucial respects, namely (i) the lack of a solid-fluid-solid evolution for any layer and, more importantly, (ii) the *half occupancy* of the fluid layer. The latter is the hallmark of the DOF state, which here therefore emerges as the likeliest explanation for RL.

3

In order to further elucidate the connection between surface melting and PR, we examined the lateral diffusion coefficient layer by layer. Mean square displacements were averaged for all particles spending time within three vertical windows corresponding to adatom layer, first layer (surface) and second layer. Not surprisingly, adatoms are very diffusive (gas-like), while buried layers are solid, and poorly diffusive. The top layer diffusivity was always sizable, but larger by about a factor two in the half-covered case, where it is similar to the surface mass transport coefficient near T_m [18] (Fig. 4). This confirms that a height jump by about half a layer across PR also takes the top layer from solid to liquid, in agreement with the GCMC analysis. Thus sudden formation of the liquid half layer at PR represents the threshold for the first appearance of the liquid, which will subsequently extend to lower layers and grow critically to a thicker liquid film as temperature is further raised to approach T_m.
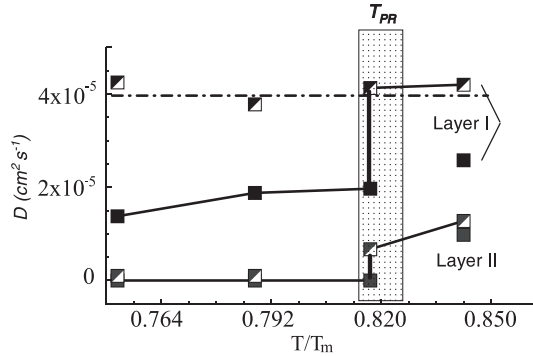

FIG. 4.   Lateral diffusion coefficient obtained for a free Ar(111) surface with half (black and white squares) and full (black squares) coverages at different temperatures. The RL onset temperature region T_{PR} is dotted. At half coverage, the top layer is always liquid; at full coverage, the top layer is still solid at T_{PR}. The second layer is always weakly diffusive, and adatoms (not shown) diffuse as a gas in every case. Solid lines guide the eye from full coverage below T_{PR} to half coverage above T_{PR}. Note the diffusion coefficient jump. Surface mass transport coefficient near T_m (from [18]) is dash-dotted.

Summarizing, our results can explain the experimental evidence of RL occurring in the adsorption of rare gas on a solid substrate. Layer by layer occupancies and direct insight on the surface processes that are not directly accessible from experiments, confirm the interpretation of the reentrant layering transition in terms of preroughening. The DOF state consists of a half monolayer of barely percolating 2D liquid islands, floating on top of a solid substrate. We found a coincidence of the onset of premelting in the top layer with a PR transition, where coverage jumps from full to partial. These two surface phenomena, apparently very different, appear here to be intimately connected. A lattice model addressing this connection has been published separately [19].

It is a pleasure to thank S. Prestipino, E. Jagla, and G.

[1] see, *e.g.*, A. C. Levi, in *Phase Transitions and Surface Films 2*, Eds H. Taub, G. Torzo, H. J. Lauter and S. C. Fain, Jr. (NATO ASI series, Series B, Physics, v. 267), p. 327; L. Pietronero and E. Tosatti, Solid State Comm. **32**, 255 (1979).

[2] H. Van Bejieren and I. Nolden, in *Structure and Dynamics of Surfaces II*, Eds. W. Schommers and P. von Blanckenhagen (Springer-Verlag, Heidelberg, 1987) p. 259.

[3] K. Rommelse and M. den Nijs, Phys. Rev. Lett. **59**, 2578 (1987); M. den Nijs and K. Rommelse, Phys. Rev. B **40**, 4709 (1989).

[4] G. B. Hess, in *Phase Transitions and Surface Films 2*, *op. cit.*, p. 357.

[5] H. S. Youn and G. B. Hess, Phys. Rev. Lett. **64**, 918 (1990), H. S. Youn, X. F. Meng and G. B. Hess, Phys. Rev. B **48**, 14556 (1993); G. B. Hess, in *Phase Transitions in Surface Films 2*, edited by H. Taub *et al.* (Plenum, New York, 1992).

[6] P. Day, M. Lysek, M. LaMadrid, and D. Goodstein, Phys. Rev. **47**, 10716 (1993).

[7] J. M. Phillips and J. Z. Larese, Phys. Rev. Lett. **75**, 4330 (1995); P. B. Weichman and D. Goodstein, Phys. Rev. Lett. **75**, 4331 (1995).

[8] P. B. Weichman, P. Day and D. Goodstein, Phys. Rev. Lett. **74**, 418 (1995).

[9] J. M. Phillips, Q. M. Zhang and J. Z. Larese, Phys. Rev. Lett. **71**, 2971 (1993); J.M. Phillips and J. Z. Larese, Phys. Rev. Lett. **75**, 4330 (1995); and Phys. Rev. B **56**, 15938 (1997).

[10] P. B. Weichman and A. Prasad, Phys. Rev. Lett. **76**, 2322 (1997).

[11] F. Rieutord, R. Simon, R. Conradt, and P. Muller-Buschbaum, *Europhys. Lett.* **37**, 565 (1997).

[12] L. A. Rowley, D. Nicholson and N. G. Parsonage, J. Comput. Phys. **26**, 66 (1975).

[13] F. Celestini, D. Passerone, F. Ercolessi and E. Tosatti, Surf. Sci. **402-404**, 886 (1998).

[14] G. E. Norman and V. S. Filipov, High Temp. (USSR) **7**, 216 (1969).

[15] X. J. Chen, F. Ercolessi, A. C. Levi and E. Tosatti, Surf. Sci **249**, 237 (1991).

[16] J. D. Weeks, Phys. Rev. B **26**, 3998 (1982).

[17] S. Prestipino, C. S. Jayanthi, F. Ercolessi, and E. Tosatti, Surf. Rev. and Lett. **4**, 843 (1997); C. S. Jayanthi *et al.*, Surf. Sci. Lett., accepted.

[18] J. Q. Broughton and G. H. Gilmer, J. Chem. Phys. **79**(1983)5119.

[19] E. A. Jagla, S. Prestipino and E. Tosatti , Phys. Rev. Lett. **83**, 2753 (1999).